

A&A 565, A82 (2014)
 DOI: [10.1051/0004-6361/201322999](https://doi.org/10.1051/0004-6361/201322999)
 © ESO 2014

**Astronomy
&
Astrophysics**

Symbiotic stars in X-rays. II. Faint sources detected with *XMM-Newton* and *Chandra*

N. E. Nuñez¹, G. J. M. Luna², I. Pillitteri³, and K. Mukai⁴

¹ Instituto de Ciencias Astronómicas de la Tierra y el Espacio (ICATE-UNSJ), Av. España (sur) 1512, 5400 San Juan, Argentina
 e-mail: nnunez@icate-conicet.gob.ar

² Instituto de Astronomía y Física del Espacio (IAFE), CC 67 – Suc. 28 (C1428ZAA) CABA, Argentina

³ Osservatorio Astronomico di Palermo (INAF), piazza del Parlamento 1, 90 134 Palermo, Italy

⁴ CRESST and X-ray Astrophysics Laboratory, NASA/GCFC, Greenbelt MD 20 771, USA. Department of Physics, University of Maryland, Baltimore County, 1000 Hilltop Circle, Baltimore MD 21 250, USA

Received 6 November 2013 / Accepted 1 March 2014

ABSTRACT

We report the detection from four symbiotic stars that were not known to be X-ray sources. These four object show a β -type X-ray spectrum, that is, their spectra can be modeled with an absorbed optically thin thermal emission with temperatures of a few million degrees. Photometric series obtained with the Optical Monitor on board *XMM-Newton* from V2416 Sgr and NSV 25735 support the proposed scenario where the X-ray emission is produced in a shock-heated region inside the symbiotic nebulae.

Key words. binaries: symbiotic – X-rays: binaries

1. Introduction

In a binary system, where a white dwarf (WD) accretes from the wind of a red giant companion and frequently forms an accretion disk, where the WD can experience frequent outbursts of different intensity, and where mass is ejected at speeds of a few hundreds km s^{-1} , it seems natural to expect that X-ray emission could be frequently detected, which originated in either the surface of the white dwarf by quasi-stable nuclear burning, the accretion disk, or shocks due to ejections of material. However, it was only recently that a significant fraction of these systems, known as WD symbiotics, was detected at X-ray wavelengths using modern instruments such as *Swift*, *XMM-Newton* or *Chandra*. In general, the emission is faint with fluxes as low as a few 10^{-14} $\text{ergs cm}^{-2} \text{s}^{-1}$. The WD symbiotics have X-ray spectra that can be classified into four types: α -type are supersoft X-ray sources whose X-ray spectrum peaks at energies lower than 0.4 keV; β -type comprises those sources with soft X-ray emission and whose spectrum extends up to energies of less than 2.4 keV; δ -type are highly absorbed, hard X-ray sources with detectable thermal emission above 2.4 keV and β/δ -type includes those WD symbiotics with two X-ray thermal components, which are soft and hard. (The details of this classification scheme are in Luna et al. 2013, hereafter Paper I).

In this paper, we present the detection at X-ray energies of four WD symbiotics: Hen 2-87, NSV 25735, V2416 Sgr, and Hen 2-104 that were observed with *XMM-Newton* and *Chandra* that were not known to be X-ray sources before. In Sect. 2, we show the details of the data reduction, while we present the results in Sect. 3. The discussion and concluding remarks are presented in Sect. 4.

2. Observations and data reductions

We searched for imaging X-ray observations that are sensitive in the 0.3–10 keV band (*ASCA*, *XMM-Newton*, *Chandra*, *Suzaku*,

and *Swift*) using the HEASARC¹ database of all the symbiotic stars listed in Belczyński et al. 2000. Excluding the symbiotic stars already known to be X-ray sources (see Paper I, which contains a complete list of known X-ray emitting symbiotic stars), we detected X-ray emission from four symbiotic stars: Hen 2-87, NSV 25735, V2416 Sgr, and Hen 2-104.

The stars Hen 2-87, NSV 25735, and V2416 Sgr were observed with *XMM-Newton*. While NSV 25735 and V2416 Sgr were the main target of the observations, Hen 2-87 was serendipitously detected at the edge of the field of view of the EPIC camera at about $10''$ away from the aim point. The *XMM-Newton* data were reprocessed using the SAS (v13.0.1) tool `emproc` and `epproc` to apply the latest calibration. All observations were obtained in full mode and with the thick filter. After filtering the event list for flaring particle background, Hen 2-87 and V2416 Sgr were evidently detected and we extracted source spectra and light curves from circular regions centered on the SIMBAD coordinates of each objects with radius of 600 or 640 pixels ($\sim 32''$) (we used a smaller region in the case of Hen 2-87 because it lies close to a detector edge). Ancillary and response matrices were created with the SAS tools `arfgen` and `rmfgen`. The background spectra and light curves of NSV 25735 and V2416 Sgr were extracted from annuli regions centered on the source with inner and outer radii of 650 and 1000 pixels, respectively. Because Hen 2-87 is located near the detector edge, we extracted the background from a off-centered circle from the source region with a $90''$ radius. Given the faintness of the sources, we combined the `pn`, `mos1` and `mos2` spectra (using the `epicspeccombine` script) by increasing the signal-to-noise of the spectra to be modeled.

To search for X-ray emission from NSV 25735, we used an algorithm based on wavelet convolution for the EPIC *XMM-Newton* images. This code is derived from the ROSAT and *Chandra* versions (see Damiani et al. 1997a and

¹ <http://heasarc.gsfc.nasa.gov/docs/archive.html>

Table 1. Observations log.

Object	Instrument	ObsID	Date	Exposure time [ks]	Offset["] ^a
Hen 2-87	<i>XMM-Newton</i> – EPIC	0109480101	2002/06/03	53	10.402
		0109480201	2002/08/26	55	10.402
		0109480401	2003/01/21	48	10.403
NSV 25735	<i>XMM-Newton</i> – EPIC	0401670201	2007/04/30	10	0.007
V2416 Sgr	<i>XMM-Newton</i> – EPIC	0099760201	2000/03/22	61	0.005
	<i>XMM-Newton</i> – OM	0099760201	2000/03/22	47	0.005
Hen 2-104	<i>Chandra</i> – ACIS	2577	2002/04/08	20	0.022

Notes. ^(a) Offset from instrument aim point, which is obtained from HEASARC.

Damiani et al. 1997b for details). The *XMM-Newton* version allows us to perform source detection on the data of the three EPIC camera simultaneously, thus improving the sensitivity of the result. The detected sources are those with a significance threshold higher than 4.5σ of the local background. This threshold is chosen on the basis of simulations of background only images, to retain one spurious source in the image at most. The star NSV 25735 is detected at a significance level of 15.22σ ; it has about 400 ± 40 counts in the sum of *pn*, *mos1*, and *mos2* images and a rate of ~ 12 counts ks^{-1} .

The stars NSV 25735 and V2416 Sgr were also observed with the optical monitor (OM) on board *XMM-Newton*. While NSV 25735 was observed in fast imaging mode with the *UVM2* filter, V2416 Sgr was observed in image mode using the *U*, *B* and *V* filters (*UVW2* and *UVM2* filters were also used but the data were corrupted). We analyzed pipeline-reduced data and looked for variability in the photometric time series. The star NSV 25735 has been observed with *Swift*/XRT/UVOT; however, the source was not detected in X-rays, and the UVOT images were saturated (see Paper I for details).

The star Hen 2-104 was observed with *Chandra* using the ACIS-S camera. We reprocessed the data using the `chandra_repro` script in CIAO² and obtained a new event file by applying the calibration version 4.5.2. Afterwards, we extracted spectra (using the `specextract` script) and light curves (using the `dmextract` script) for the source and background. Source products were extracted from a circular region (centered on the SIMBAD³ coordinates) with 100 pixels ($\sim 50''$) radius while background spectra and light curves were extracted from three circular regions of 160 pixels ($\sim 80''$) each. The response and ancillary matrices were created using the `mkrmf` and `mkarf` scripts. All the details of the observations are found in Table 1.

We fit the unbinned spectra using XSPEC⁴, and because it is not appropriate to use the χ^2 statistic to fit the spectra of sources with a low numbers of counts, such as the ones studied here, we use the C-statistic (Cash 1979). All errors in the fit parameters were estimated at 90% confidence. To evaluate the number of components are needed in the spectral model, we use the likelihood ratio test as described by Protassov et al. (2002) and implemented it in XSPEC through the `lrt` script. This test compares the statistics (Cstat) of the complex and simple model in *N* sets of simulated data and helps us to evaluate the statistical significance of adding one or more components into a single-component model.

² <http://xcx.cfa.harvard.edu/ciao/index.html>

³ <http://simbad.u-strasbg.fr/simbad/sim-fid>

⁴ <http://heasarc.gsfc.nasa.gov/docs/xanadu/xspec/>

3. Results

By correlating the existing catalog of Belczyński et al. (2000) with the HEASARC database, we found X-ray emission from four symbiotic stars observed with *XMM-Newton* and *Chandra*. Their low X-ray fluxes (see Table 2) explain why these sources were not detected before. Given the limited statistical quality of these X-ray data, we limit ourselves to spectral models that have been successfully used for other symbiotic stars. All of them show a soft optically thin thermal X-ray spectrum with emission that peaks around 1 keV and does not extend to very high energies. This is sufficient to fit their spectra and classify them as β -type in the scheme whose details are found in Paper I (in the next subsections we detail the fit procedure for each object). We also tried to fit the X-ray spectrum with non-thermal models, which were discarded because they yielded unrealistic values for the fit parameters.

For all sources, we show the classification based on infrared (IR) colors proposed by Webster & Allen (1975) and refined by Allen (1984), where S-type systems emit IR radiation typical of red giant atmospheres (M-type). These systems are relatively dust-free and have binary periods shorter than 20 years. The D-type systems show IR emission indicative of dust; that is, they have a thermal radiation with average temperatures of 1000 K, which generally contain Mira variables as companions and have binary periods longer than 10 years. This is similar to R Aqr, which shows a period of 46 years (Gromadzki & Mikołajewska 2009). The D'-type systems have very red colors in the far IR and a cool companion of spectral types F or G. The IR type of all objects was extracted from Table 1 in Belczyński et al. (2000).

3.1. Hen 2-87

This object is classified as S-type. Little is known about this source and there is no recorded outburst in the literature. The star Hen 2-87 was detected in three *XMM-Newton* observations in the field of WR 47 (see Table 1). Given that the source was detected at a higher count rate during ObsID 0109480401 (hereafter 401) taken in 2003 ($0.037 \pm 0.001 \text{ s}^{-1}$, as compared to $0.011 \pm 0.002 \text{ counts s}^{-1}$ during ObsID 0109480201 (hereafter 201) and $0.013 \pm 0.002 \text{ counts s}^{-1}$ for ObsID 0109480101 (hereafter 101)), we fit this spectrum and then used the accepted model to fit the other two datasets. We first fit the spectrum with an absorbed optically thin thermal plasma (`wabs×apec`), but there were important residuals in the $E \gtrsim 2$ keV region. Then, we added a second optically thin thermal component, which is also affected by the same absorber than the previous component (`wabs×(apec1+apec2)`), and the fit showed a much more uniform distribution of the residuals. As explained in Sect. 2, we used the `lrt` to assess the statistical significance of adding

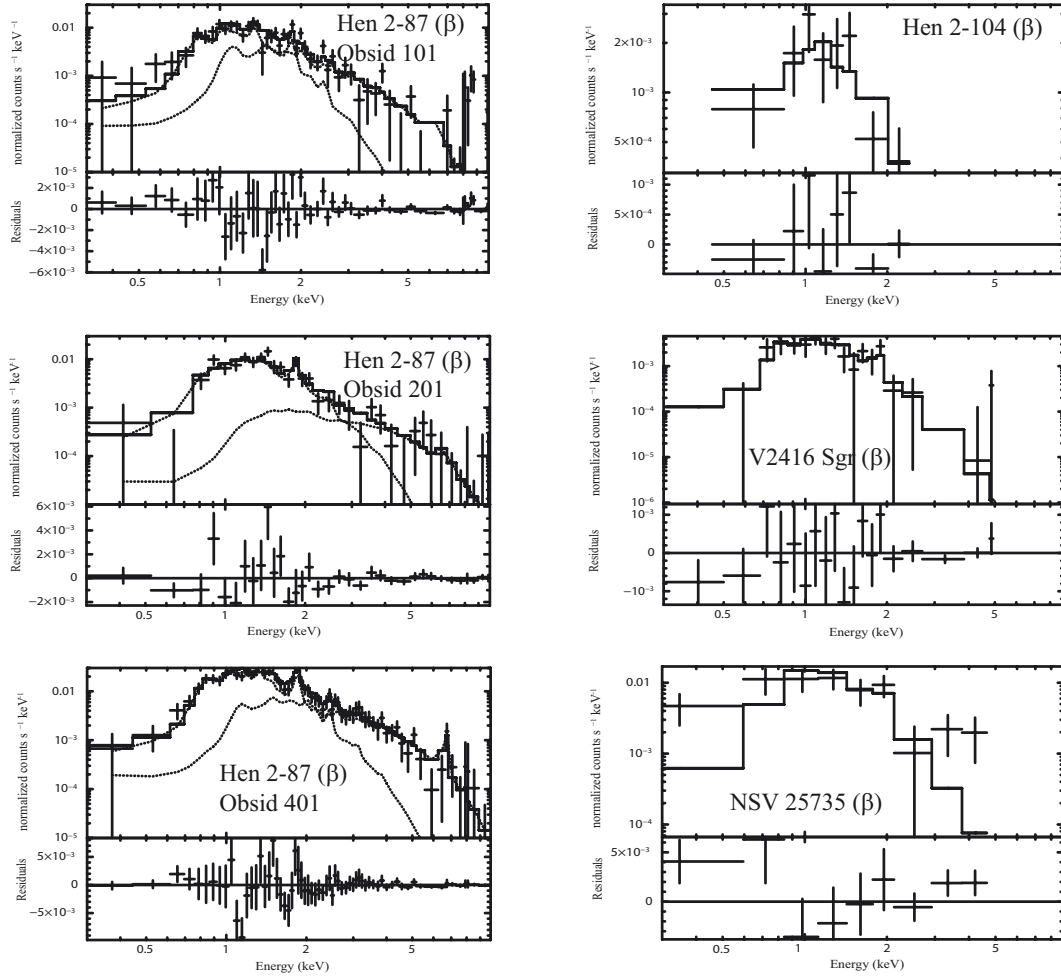


Fig. 1. *Chandra* and *XMM-Newton* X-ray spectra of the WD symbiotic with newly discovered X-ray emission with their X-ray spectral types: Hen 2-87, Hen 2-104, V2416 Sgr, and NSV 25735. We show the three spectra obtained with *XMM-Newton* from Hen 2-87. The full line shows the best-fit model described in Sect. 3, while the dotted line shows the contribution of the individual spectral components in the case of multi-component models. The X-ray spectral classification for each source is included between parentheses in each panel.

this second component, and after 1000 simulations, 60% of them showed an improvement in the statistic. The addition of the second component has a low significance; however, given that this component describe the high energy part of the spectrum, we find plausible to keep it in our model (see Fig. 3). We retain this complex model throughout the analysis, which could be better tested in more sensitive observations. During the three observations, the plasma temperatures and the absorbing column have commensurate values. The flux, on the other hand, almost doubled from ObsID 101 to 401 (see Table 2).

3.2. NSV 25735

The symbiotic NSV 25735 is classified as D'-type. The system contains a WD with moderate temperature ($T \sim 50\,000$ K, Schmid & Nussbaumer 1993). The cool companion star has three different spectral type determinations in the literature: G5 (Mürset & Schmid 1999), G4 III/IV (Smith et al. 2001), and G7 III (Munari et al. 2001), which suggests a T_{eff} in a range between 5025–5300 K. The cool component is rotating at a spectacular speed of 105 km s^{-1} , unseen in field G-type giants (Munari et al. 2001). As only seven D'-type symbiotic are known, the results about the three sources (HD 330036, AS 201, and NSV 25735) studied so far with high resolution

optical spectroscopy show rapid rotation and *s*-process elemental overabundances, which might indicate that these two traits are signatures of these symbiotic systems (Jorissen et al. 2005). Moreover, NSV 25735 is the first D'-type symbiotic to show jets. Munari et al. (2001) analyzed the $H\alpha$ profile and found a central component (that remained constant for months) and two weaker, symmetrically placed components at both sides of the profile. These two components show large day-to-day variability (velocity and width), which are spectral signatures of jet-like discrete ejection events. The authors also derived a high orbital inclination of 60° ; therefore the de-projected velocity of the jet components must be much larger than the observed velocity shifts (150 km s^{-1}) and well in excess of the escape velocity from the companion (1000 km s^{-1}). The jet components are also visible in the profiles of He I lines with a velocity of 300 km s^{-1} . There are not recorded outbursts but the bipolar mass outflow is highly variable (Munari et al. 2001). The very fast rotation, which has been proposed and explained by Jeffries & Stevens (1996), is a mechanism in which the accretion of a slow massive wind from the AGB progenitor of the current WD can transfer sufficient angular momentum and spin up the companion, which is analogous with millisecond radio pulsars (van den Heuvel & Bonsema 1984). This also explains the chemical enrichment in *s*-process elements in D'-type symbiotic systems that were present in the AGB wind (Pereira et al. 2005).

Table 2. X-ray spectral fitting results.

Object	Model	kT [keV]	N_{H} [10^{22} cm $^{-2}$]	F_{X}	L_{X}
Hen 2-87(101)	wabs \times (apec $_1$ +apec $_2$)	1: $0.4^{+0.4}_{-0.2}$	$1.3^{+0.2}_{-0.2}$	$7.5^{+0.9}_{-0.9}$	$9.0^{+0.7}_{-0.7}$
		2: $1.9^{+0.9}_{-0.4}$			
Hen 2-87(201)	wabs \times (apec $_1$ +apec $_2$)	1: $0.7^{+0.2}_{-0.1}$	$1.2^{+0.2}_{-0.2}$	$8.1^{+1.1}_{-1.1}$	$9.7^{+1.3}_{-1.3}$
		2: ≥ 2.0			
Hen 2-87(401)	wabs \times (apec $_1$ +apec $_2$)	1: $0.6^{+0.1}_{-0.1}$	$1.4^{+0.1}_{-0.1}$	14^{+1}_{-1}	$20.0^{+2.2}_{-4.4}$
		2: $3.0^{+1.0}_{-1.0}$			
NSV 25735	wabs \times apec	$0.7^{+0.3}_{-0.3}$	$1.2^{+0.4}_{-0.4}$	9^{+3}_{-3}	3^{+2}_{-1}
V2416 Sgr	wabs \times apec	$0.5^{+0.2}_{-0.2}$	$1.1^{+0.3}_{-0.2}$	$0.9^{+0.2}_{-0.2}$	$1.1^{+0.2}_{-0.3}$
Hen 2-104	wabs \times apec	≥ 1.5	≤ 0.3	$0.3^{+0.1}_{-0.1}$	$4.2^{+1.0}_{-1.5}$

Notes. X-ray flux (F_{X}) and luminosity (L_{X}) in units of 10^{-13} ergs s $^{-1}$ cm $^{-2}$ and 10^{31} ergs s $^{-1}$ respectively, are calculated in the 0.3–10.0 keV energy band.

The X-ray spectrum obtained with *XMM-Newton*, which extends up to energies of ~ 5 keV, can be modeled using an absorbed ($N_{\text{H}} = 1.2^{+0.4}_{-0.4} \times 10^{22}$ cm $^{-2}$) optically thin thermal plasma with a temperature $kT = 0.7^{+0.3}_{-0.3}$ keV. The *XMM-Newton* detected 351 source counts; therefore, the model parameters cannot be constrained by the fit (see Table 2). The unabsorbed flux in the 0.3–10.0 keV energy band is $F_{\text{X}} = 9^{+3}_{-3} \times 10^{-13}$ ergs cm $^{-2}$ s $^{-1}$ and the corresponding luminosity at a distance of 575 pc (Munari et al. 2001) is $L_{\text{X}} = 3^{+2}_{-1} \times 10^{31}$ ergs s $^{-1}$.

3.3. V2416 Sgr

This object was classified as a S-type symbiotic. The *XMM-Newton* detected 220 counts from this source. The X-ray spectrum can be modeled with an absorbed ($N_{\text{H}} = 1.1^{+0.3}_{-0.2} \times 10^{22}$ cm $^{-2}$) optically thin thermal plasma (with $kT = 0.5^{+0.2}_{-0.2}$ keV). It is interesting to note that the value of N_{H} that could be inferred (using the relation between N_{H} and $E(B - V)$ that is proposed by Groenewegen & Lamers 1989). From the published reddening values of $E(B - V) = 1.7$ this is 4.4×10^{22} cm $^{-2}$ (Luna & Costa 2005), or by using $E(B - V) = 2.5$ (Mikolajewska et al. 1997), we have $N_{\text{H}} = 6.6 \times 10^{22}$ cm $^{-2}$. Both values are much higher than the value found from our fit of the X-ray spectrum. On the other hand, Whitelock & Munari (1992) calculated a lower value of $E(B - V) \sim 0.13$; at the same time, they mentioned that the colors of this star suggest it experiences several magnitude more extinction than the value derived. This suggest that the X-ray emitting region could be located in the outer parts of the symbiotic nebulae, where column density and absorption are smaller. The unabsorbed flux in the 0.3–10.0 keV energy band is $F_{\text{X}} = 0.9^{+0.2}_{-0.2} \times 10^{-13}$ ergs cm $^{-2}$ s $^{-1}$ and the corresponding luminosity at a distance of 1.0 kpc (the actual distance is unknown) is $L_{\text{X}} = 1.0^{+0.2}_{-0.2} \times 10^{31}$ ergs s $^{-1}$.

The OM light curves from V2416 Sgr and NSV 25735 show a small fractional variability $\lesssim 3\%$ (which we calculate as the observed variance over the average count rate), which is expected for their β X-ray spectral type. In the diagram presented in Paper I (Fig. 7), where the hardness of the X-ray spectrum is plotted against the fractional UV variability, can be seen a separation between those systems that are accretion-powered and those that are powered by quasi-stable shell burning. The stars NSV 25735 and V2416 Sgr are located in the lower left corner; in the region of systems, where the WDs are powered by quasi-stable shell burning.

3.4. Hen 2-104

The star Hen 2-104 is classified as a D-type symbiotic. Its extended nebula has an hourglass shape, extending $75''$ (Schwarz et al. 1989). More detailed studies show that the nebula around Hen 2-104 consists of nested hourglass-shaped structures (with the inner structure extending $\sim 12''$ while the outer structure extends for $\sim 80''$) and a collimated polar jet (see Fig. 1 in Corradi et al. 2001). The outer pair of lobes and jets are produced by a high-velocity outflow from the WD companion of the Mira, while the inner, slowly expanding lobes are produced by the Mira wind itself (Corradi et al. 2001). The densities range from $n_{\text{e}} = 500$ cm $^{-3}$ to 1000 cm $^{-3}$ in the inner lobes and from 300 cm $^{-3}$ to 500 cm $^{-3}$ in the outer lobes (Santander-García et al. 2008).

The *Chandra* observation was already studied by Montez et al. (2006). Due to poor astrometry, they mistakenly attributed the X-ray emission to a region heated by shocks and displaced $2''$ SE from the central symbiotic system (R. Montez, priv. comm.). Our new data analysis shows that the X-ray emission is concentrated in the central region of the nebula. The faint X-ray emission can be modeled with an absorbed ($N_{\text{H}} \lesssim 0.3 \times 10^{22}$ cm $^{-2}$) optically thin thermal plasma (with $kT \gtrsim 1.5$ keV); however, we are not able to constrain due to the low number of counts detected (42) further the value of the model parameters. Upper or lower limits are listed in Table 2. The unabsorbed flux in the 0.3–10.0 keV energy band is $F_{\text{X}} = 0.3^{+0.1}_{-0.1} \times 10^{-13}$ ergs cm $^{-2}$ s $^{-1}$ and the corresponding luminosity at a distance of 3.3 kpc (Santander-García et al. 2008) is $L_{\text{X}} = 4.2^{+1.0}_{-1.5} \times 10^{31}$ ergs s $^{-1}$.

4. Discussion and conclusions

We found X-ray emission from four WD symbiotics that were not known to be X-ray sources. The X-ray emission from all of them can be classified as β -type, following the scheme originally proposed by Mürset et al. (1997) and recently updated in Paper I. Our results confirm that β -type X-ray emission is the most frequent among the WD symbiotic, which increases the number of known β -type sources to 16 out of 48 symbiotic with X-ray emission. The X-ray emission from the new sources is faint with luminosities that have an average of 10^{31} ergs s $^{-1}$ (albeit the uncertainties in their distance), which explains why pointing, dedicated observations were necessary for their detection. For β -type systems, their X-ray emission seems to be

associated with shocks in the nebulae that could originate in a colliding wind region or inside extended jets (known to be present in NSV 25735 and Hen 2-104).

Although most models of colliding-wind scenarios require that the WD in the system undergo a recent outburst to trigger a fast, tenuous wind, the β -type systems presented here and those presented in Paper I do not have any recent outbursts recorded. While α or δ type X-ray spectra are directly linked to the source that powers the WD, which includes shell-burning or accretion, β type X-ray emission is not. The absence of strong variability, with a β -type X-ray spectrum strongly suggest that the observed X-rays do not originate in the accretion disk around the WD, while soft X-rays are too energetic to be originate in a shell-burning WD. Our physical picture is that, nuclear burning could lead to a strong wind from the WD (or the accretion disk near the WD in these systems), which collides with the wind from the cool star and leads to observed soft X-ray emission. Super-soft X-ray emission from the WD might also be present but it would be absorbed by the dense symbiotic nebula.

Using the temperature obtained from spectral models of these sources (0.4 keV to ~ 2.0 keV) and assuming strong shock conditions, we can derive a shock speed, v_{shock} . We obtain v_{shock} in the range of ~ 1000 to ~ 2500 km s $^{-1}$. Similar speeds are observed in the β -type sources presented in Paper I and Müersset et al. (1997) and are roughly consistent with the speeds of X-ray emitting outflows from WD symbiotic (Nichols et al. 2007; Galloway & Sokolowski 2004). High outflow speeds of a few thousands km s $^{-1}$ have been observed in the optical line profiles of MWC 560 (Schmid et al. 2001), although they are not consistent with the temperatures observed from the β component in its X-ray spectrum (Stute & Sahai 2009). The disparity between the X-ray inferred speed and speeds from optical line widths has also been observed in the diffuse X-ray emission from planetary nebulae (Soker & Kastner 2003). In the dense symbiotic nebula, however, some authors have modeled the observed UV line profiles of O VI and He II as due to electron scattering (Sekeráš & Skopal 2012a,b). Lee (2000) proposed that Ramman scattering might be responsible for the broad H α line wings observed in symbiotics.

The number of known symbiotics with X-ray emission is rapidly increasing with the availability of new instruments, and it is expected to increase even more with more sensitive instruments and deeper surveys (e.g., NuSTAR⁵ and eROSITA⁶). We now know 48 systems with X-ray emission that originates in four different scenarios. With this number of sources, it seems timely to study their statistical properties. Is there any trend or relationship between IR and X-ray spectral types? In the symbiotic stars catalog of Belczyński et al. (2000), 63% of the objects (139) are classified as S-type, 15% (34) as D-type, and 3% (7) as D'-type. Among the 48 symbiotics with X-ray emission, 33% of them have a β -type X-ray spectrum. Roughly half of the β -type symbiotics have IR S-type spectrum, while 25% have D-type,

6.3% have D'-type; and 6.3% do not have classification. We did not find any clear tendency or correlation between IR and X-ray types, that is, the fractions of IR types are roughly similar among X-ray emitting symbiotics and those with no X-ray emission detected.

Acknowledgements. We thank Jennifer L. Sokolowski for useful discussions about X-ray emission from symbiotic stars. N.E.N. acknowledge Consejo Nacional de Investigaciones Científicas y Técnicas, Argentina (CONICET) by the Postdoctoral Fellowship. G. J. M. Luna acknowledges funding from grants PICT/2011/269 from Agencia and PIP D-4598/2012 from Consensus National de Investigación Científicas y Técnicas, Argentina. This research has made use of data obtained from the High Energy Astrophysics Science Archive Research Center (HEASARC), provided by NASA's Goddard Space Flight Center; and the Vizier catalogue access tool, CDS, Strasbourg, France. The original description of the Vizier service was published in Ochsenbein et al. (2000).

References

- Allen, D. A. 1984, *PASA*, 5, 369
 Belczyński, K., Mikołajewska, J., Munari, U., Ivison, R. J., & Friedjung, M. 2000, *A&AS*, 146, 407
 Cash, W. 1979, *ApJ*, 228, 939
 Corradi, R. L. M., Livio, M., Balick, B., Munari, U., & Schwarz, H. E. 2001, *ApJ*, 553, 211
 Damiani, F., Maggio, A., Micela, G., & Sciortino, S. 1997a, *ApJ*, 483, 350
 Damiani, F., Maggio, A., Micela, G., & Sciortino, S. 1997b, *ApJ*, 483, 370
 Galloway, D. K., & Sokolowski, J. L. 2004, *ApJ*, 613, L61
 Groenewegen, M. A. T., & Lamers, H. J. G. L. M. 1989, *A&AS*, 79, 359
 Gromadzki, M., & Mikołajewska, J. 2009, *A&A*, 495, 931
 Jeffries, R. D., & Stevens, I. R. 1996, *MNRAS*, 279, 180
 Jorissen, A., Začs, L., Udry, S., Lindgren, H., & Musaev, F. A. 2005, *A&A*, 441, 1135
 Lee, H.-W. 2000, *ApJ*, 541, L25
 Luna, G. J. M., & Costa, R. D. D. 2005, *A&A*, 435, 1087
 Luna, G. J. M., Sokolowski, J. L., Mukai, K., & Nelson, T. 2013, *A&A*, 559, A6
 Mikołajewska, J., Acker, A., & Stenholm, B. 1997, *A&A*, 327, 191
 Montez, Jr., R., Kastner, J. H., & Sahai, R. 2006, in *Am. Astron. Soc. Meet. Abstr.*, BAAS, 38, 1029
 Müersset, U., Wolff, B., & Jordan, S. 1997, *A&A*, 319, 201
 Munari, U., Tomov, T., Yudin, B. F., et al. 2001, *A&A*, 369, L1
 Müersset, U., & Schmid, H. M. 1999, *A&AS*, 137, 473
 Nichols, J. S., DePasquale, J., Kellogg, E., et al. 2007, *ApJ*, 660, 651
 Ochsenbein, F., Bauer, P., & Marcout, J. 2000, *A&AS*, 143, 23
 Pereira, C. B., Smith, V. V., & Cunha, K. 2005, *A&A*, 429, 993
 Protassov, R., van Dyk, D. A., Connors, A., Kashyap, V. L., & Siemiginowska, A. 2002, *ApJ*, 571, 545
 Santander-García, M., Corradi, R. L. M., Mampaso, A., et al. 2008, *A&A*, 485, 117
 Schmid, H. M., & Nussbaumer, H. 1993, *A&A*, 268, 159
 Schmid, H. M., Kaufer, A., Camenzind, M., et al. 2001, *A&A*, 377, 206
 Schwarz, H. E., Aspin, C., & Lutz, J. H. 1989, *ApJ*, 344, L29
 Sekeráš, M., & Skopal, A. 2012a, *Baltic Astron.*, 21, 196
 Sekeráš, M., & Skopal, A. 2012b, *MNRAS*, 427, 979
 Smith, V. V., Pereira, C. B., & Cunha, K. 2001, *ApJ*, 556, L55
 Soker, N., & Kastner, J. H. 2003, *ApJ*, 583, 368
 Stute, M., & Sahai, R. 2009, *A&A*, 498, 209
 van den Heuvel, E. P. J., & Bonsema, P. T. J. 1984, *A&A*, 139, L16
 Webster, B. L., & Allen, D. A. 1975, *MNRAS*, 171, 171
 Whitelock, P. A., & Munari, U. 1992, *A&A*, 255, 171

⁵ <http://www.nustar.caltech.edu/>

⁶ <http://www.mpe.mpg.de/eROSITA>